Available online at www.sciencedirect.com
SCIENCE DIRECT
Journal of Catalysis 230 (2005) 195–203
JOURNAL OF CATALYSIS
www.elsevier.com/locate/jcat

High-pressure X-ray photoelectron spectroscopy of palladium model hydrogenation catalysts. Part 2: Hydrogenation of *trans*-2-pentene on palladium

D. Teschner [a,b,*], A. Pestryakov [a], E. Kleimenov [a], M. Hävecker [a], H. Bluhm [a], H. Sauer [a], A. Knop-Gericke [a], R. Schlögl [a]

[a] *Fritz-Haber-Institut der MPG, Faradayweg 4-6, D-14195 Berlin, Germany*
[b] *Institute of Isotope & Surface Chemistry, CRC, Hungarian Academy of Sciences, PO Box 77, Budapest, H-1525 Hungary*

Received 2 September 2004; revised 26 November 2004; accepted 29 November 2004

Available online 13 January 2005

Abstract

We have performed the first "high-pressure" X-ray photoelectron spectroscopy (XPS) study on the palladium, hydrogen, and olefin (*trans*-2-pentene) system to gain better insight into the hydrogenation reaction. We report here data collected with the use of a Pd(111) single crystal and a polycrystalline foil. Hydrogenation was observed on polycrystalline foil (RT and 373 K) but not on Pd(111) single crystal, as revealed by on-line mass spectrometry. We observed the reaction in the presence of a huge amount of carbon (up to 73%) in the information depth of XPS. Mainly graphite was present on Pd(111), whereas other components, *C–H* and *C–Pd*, were also formed on the foil to a much greater extent. *C–Pd* characterizes a carbon species in the interaction with palladium, whereas *C–H* represents hydrogenated carbon, including chemisorbed species. The *d*-band of the foil showed a remarkable upshift toward E_{FERMI} compared with Pd(111). We concluded that the differences found in the valence and the C1*s* region are indicators of different electronic structures that contribute to the variation in activity. The palladium foil lost its activity at an elevated temperature (523 K), most probably because of desorption of hydrogen. From additional UPS measurements, we concluded that *trans*-2-pentene is hydrogenated in σ-bonded chemisorption modus, at least in UHV conditions.

Keywords: High-pressure XPS; Palladium; Hydrogenation; Carbonaceous deposits; *d*-band; UPS

1. Introduction

Group 8 transition metals play an important role in heterogeneous catalytic processes. Palladium, as one of the Group 8 metals, is widely employed in industrial processes [1–7], but also in basic research [8–23], mainly as a hydrogenation catalyst. Its interaction with various gases has been extensively investigated with regard to its catalytic [8–12,14,15,17] and surface [13,16,18–23] properties.

Most of the mechanistic studies on alkene hydrogenation have focused on the reaction of ethylene. There is little information in the literature about hydrogenation involving higher hydrocarbons. The first hydrogenation model, proposed in 1934, involved stepwise addition of surface hydrogen to σ-bonded ethylene [24]. Fifty years later, π-bonded ethylene was postulated to be the intermediate of hydrogenation on Pt surfaces [25]. Recent results from in situ spectroscopic methods, namely sum frequency generation, supported this model [26]. In recent years the involvement of surface hydrogen in hydrogenation has often been questioned, and the role of subsurface hydrogen has been pointed out by several authors [21,27,28].

Also of great interest is the effect of carbonaceous species present on the catalyst surface during the catalytic reaction. First, carbon was assumed just to block surface sites, thus leading to deactivation. Later, however, investigations of the "coke selectivity" of different hydrocarbon reactions

* Corresponding author. Fax: +49 30 8413 4676.
E-mail address: teschner@fhi-berlin.mpg.de (D. Teschner).

0021-9517/$ – see front matter
doi:10.1016/j.jcat.2004.11.035

attributed the enhanced selectivity of nondegradative transformations to the formation of carbonaceous adsorbates that prevent the excessive dehydrogenation of the surface intermediates [29–35]. Various carbon species have been observed on the surface of catalysts, ranging from carbides to hydrogen-rich aliphatic polymers. The chemical state of accumulated carbonaceous species on model palladium surfaces was often a matter of debate [36–40]. The majority of these studies were performed ex situ or in UHV conditions, far from real catalytic conditions (pressure gap).

To arrive at a comprehensive understanding of surface catalytic reaction mechanisms and to identify the factors that govern the activity and selectivity of catalysts, the structural and surface properties of catalysts should be investigated under real, working conditions. Furthermore, spectroscopic and structural characterization should be combined with online catalytic reaction analysis.

X-ray photoelectron spectroscopy (XPS) is one of the most commonly used surface science techniques; it is very powerful because of its surface sensitivity. In the first part of our paper we demonstrated the importance of gathering spectroscopic informations under relevant (if possible non-UHV) conditions. In the present part, we report on the first "high-pressure" XPS study of the hydrogenation reaction on palladium (foil and single crystal), that is, the hydrogenation of *trans*-2-pentene (t-2-p). The in situ measurements provide better insight into the hydrogenation reaction.

2. Experimental

For experimental details see Part I. Briefly, C1*s*, Pd3*d*, and valence band spectra were recorded at normal electron emission. Photon energies of $h\nu = 380$, 660, and 720 eV were chosen for the excitation of the valence band and the C1*s* and Pd3*d* core levels, respectively. This ensured that the transmission function of the electrostatic lens system did not have to be considered since electrons with the same kinetic energies were analyzed and that similar information depth was probed for Pd3*d*, C1*s*, and VB spectra (inelastic mean free path ∼ 9–13 Å). However, higher photon energies were also applied for depth profiling (1160 eV for C1*s*; inelastic mean free path ∼ 24 Å), thus providing information on the different surface species along the surface normal. The binding energies were calibrated against the Fermi level of the samples. A Pd(111) single crystal and polycrystalline palladium foil (Goodfellow, purity 99.99%) were investigated in this study. (Measurements were also carried out on 1% Pd/Al_2O_3 catalysts, but the highly insulating support caused differential charging to such an extent that we were not able to analyze the data.) The hydrogen and *trans*-2-pentene (t-2-p) gas flow into the reaction cell was controlled with calibrated mass flow controllers. A mixture of 0.6 mbar H_2 and 0.2 mbar t-2-p was introduced, and the temperature was varied in the range from RT to 523 K. *trans*-2-Pentene was supplied by Sigma–Aldrich (purity 99%) and was purified by several freeze-pump-thaw cycles before the measurements. Gas-phase analysis was carried out with a quadrupole mass spectrometer, which was mounted in the second differential pumping stage of the electrostatic lens system, where the pressure was $\sim 10^{-6}$ of the pressure in the experimental cell.

He I UPS (excitation energy 21.2 eV) measurements were carried out in a conventional UHV surface-science chamber. *trans*-2-Pentene was adsorbed to Pd(111) at 100 K. Multilayer adsorption was achieved by the introduction of 50 Langmuir of t-2-p (ionization gauge sensitivity corrected). Spectra were measured at different temperatures, from a temperature of 100 K increased stepwise to RT.

HRTEM investigations were performed in a Philips CM200 FEG electron microscope operated at 200 keV. The microscope was equipped with a Gatan imaging filter (GIF 100) and a Gatan slow-scan camera to enhance the contrast in the images. A cross-sectional specimen was prepared from a piece of Pd foil that was previously used in the in situ XPS cell in the hydrogenation of 1-pentyne.

3. Results

As already discussed in Part 1, the palladium samples quickly become contaminated by carbonaceous deposits right after some cleaning treatments because of the high base pressure (10^{-7} mbar) in our experimental cell and partly because of a beam-enhanced carbon accumulation. Nevertheless, under real-life conditions in catalytic reactors, the surface of the catalyst is most likely never ideally clean, as it is in UHV surface science studies. Moreover, the surface quickly adapts to the reaction conditions, and the carbonaceous species undergo a massive transformation as pentene is introduced to the gas phase (see later).

Since the incident X-ray beam only irradiates not only the sample surface but also the gas phase molecules in front of the sample, the in situ XP spectra show gas-phase peaks alongside the surface peaks. The binding energy (BE) scale in our figures is referenced to the Fermi level of the Pd samples, and therefore the apparent BEs of the gas-phase peaks are shifted by the amount of the work function of the sample (∼ 4.4 eV) relative to literature values, which are conventionally referenced to the vacuum level. Since the vacuum level of the gas phase depends on the vacuum level of the surrounding surfaces (especially that of the sample, since the sample surface is the closest to the detected gas-phase volume), changes in the sample work function have an influence on the gas-phase peak positions [41]. Small shifts in the gas-phase BE position throughout our spectra are therefore a reflection of changes in the work function of the sample surface [42]. Fig. 1 shows the C1*s* spectrum of gas-phase *trans*-2-pentene. At this point the sample was retracted, so that only the gas phase was measured. The spectrum shows a clear shoulder at the low-BE side and is asymmetrically broadened at the high-BE side. The first rough least-squares fit revealed that at least four peaks are needed to adequately

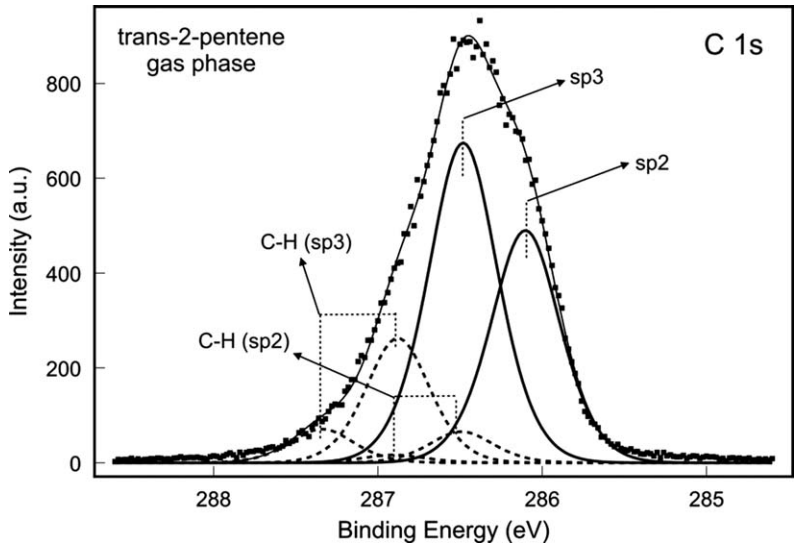

Fig. 1. C1*s* spectrum of gas-phase *trans*-2-pentene, $h\nu = 660$ eV. (···) measured data; (—) adiabatic ionisation; and (- - -) C–H stretching modes.

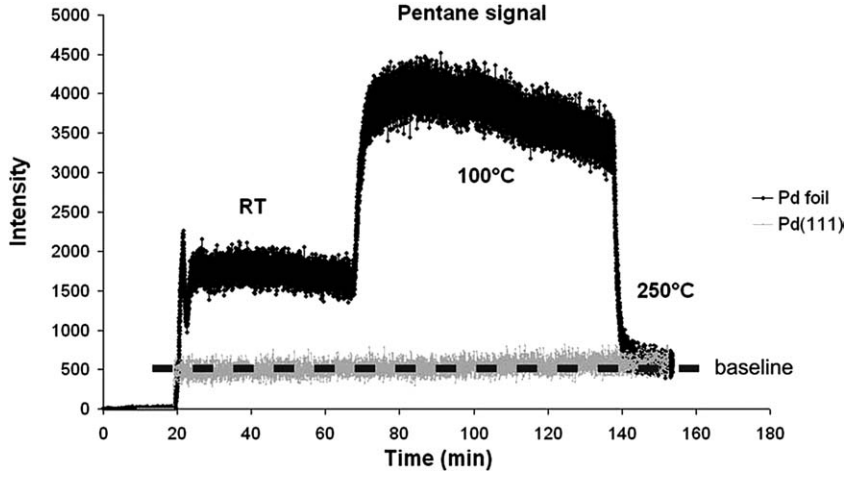

Fig. 2. Pentane signal (MS data) in the hydrogenation of *trans*-2-pentene on Pd foil and on Pd(111). H_2 (0.6 mbar) was introduced first followed by t-2-p (0.2 mbar) at min. 20 (RT). Temperature was increased to 373 K at min. 70 and increased further to 523 K at min. 140.

match the measured curve. The first two, main peaks could correspond to the adiabatic ionization of the two different C1*s* carbon types, in the sp^3 and sp^2 hybridization states. The other two peaks could be due to vibrational excitations [43]. According to the energy separation and the intensity ratios, they could be related to the C–H stretching modes of the sp^3 carbon atoms with vibrational quantum numbers 1 and 2. However, if we consider that C(sp^2)–H stretching is also present and assume statistical C(sp^3)–H/C(sp^2)–H stretching intensity ratios, the fitting analysis provides the picture shown in Fig. 1. The sp^3/sp^2 intensity ratio calculated from the peak fitting is 57 vs 43%, which is in good agreement with the expected 3:2 ratio.

The hydrogenation of t-2-p over the two palladium samples was measured in our high-pressure XPS setup. The pentane MS response is plotted in Fig. 2 as a function of reaction time at three reaction temperatures. For both samples hydrogen (0.6 mbar) was introduced first. After 20 min 0.2 mbar t-2-p was introduced. The sample temperature was increased to 373 K after 70 min and to 523 K after 140 min. We observed catalytic activity for the Pd foil sample already at room temperature. The foil reached its maximum activity at ∼ 373 K. At 523 K the foil was no longer active, as can be seen from a comparison with the amu "62" baseline. The pentene response (not shown) also reveals no additional pathway at 523 K. In contrast to the Pd foil, the Pd(111) single crystal showed no measurable activity any temperature, although the apparent surface area of the foil and the single crystal were comparable. The inactivity of the single crystal is in line with the TDS results of Doyle et al. [44], obtained under UHV conditions.

Simultaneously with the mass spectrometric analysis, the surface of the samples was measured by XPS. Figs. 3 and 4 display the corresponding C1*s* spectra. With pentene in the gas mixture we see a new peak to compare with the spectra presented in Part 1. This peak at ∼ 286.2 eV corresponds

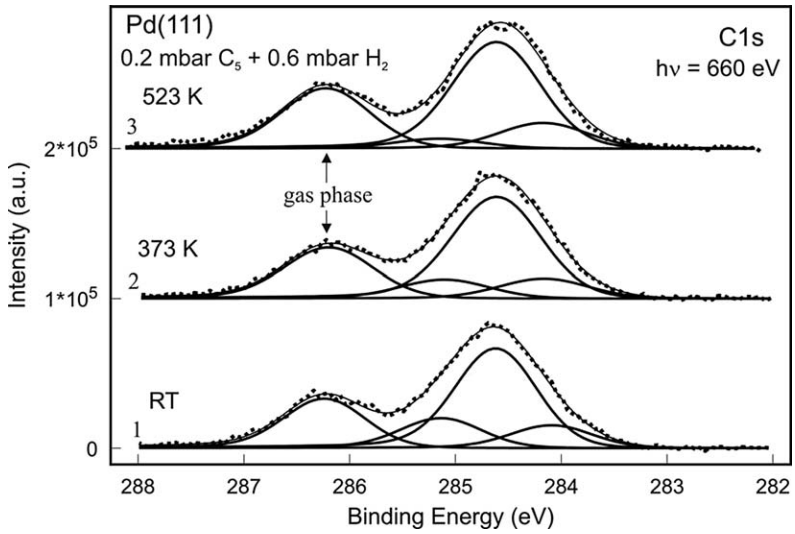

Fig. 3. C1*s* region of Pd(111) single crystal in the reaction mixture of 0.6 mbar H_2 + 0.2 mbar t-2-p at 3 temperatures (RT, 373, and 523 K). Incident photon energy, $h\nu = 660$ eV. (- - -) measured data; (—) fits. The reason for the different height of the gas phase peak is described in [45].

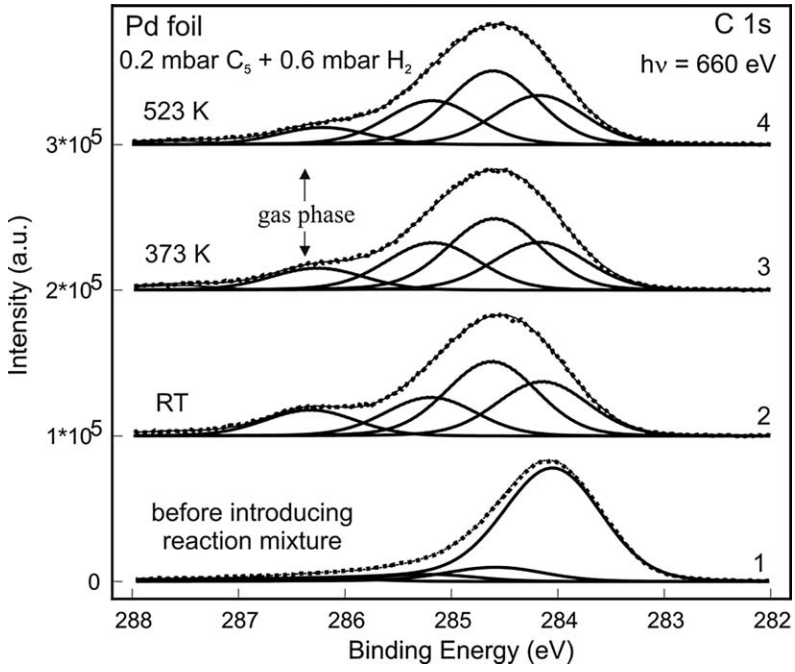

Fig. 4. C1*s* region of Pd foil in the reaction mixture of 0.6 mbar H_2 + 0.2 mbar t-2-p at 3 temperatures (RT, 373, and 523 K). The spectrum before introducing the reaction mixture is also included. Incident photon energy, $h\nu = 660$ eV. (- - -) measured data; (—) fits. The reason for the different height of the gas phase peak is described in [45].

to the gas-phase spectra as in Fig. 1. For the sake of simplicity, the gas phase was fitted here just by one peak (not as in Fig. 1). (Concerning the different height of the gas-phase peak, please read paragraph [45] in the references.) For the least-squares analysis the same surface components were used as discussed in Part 1, with the three types of carbon carbon connected to palladium (C–Pd; 284.1 eV), carbon connected to carbon (C–C; 284.55 eV), and carbon connected to hydrogen (C–H; 285.2 eV). Similar to the observation described in Part 1 for the measurements in H_2 and high vacuum, in the reaction mixture much less carbon was found on the single crystal, and the dominant part of the carbon was also graphitic (*C–C*). When the temperature was increased the C–H component on the single crystal decreased (Fig. 3, curves 2 and 3), until it almost vanished at 523 K. An opposite tendency was found for C–Pd. Its abundance was the highest at 523 K, whereas the total amount of surface carbon was at its lowest at 523 K. These tendencies are quite similar to the hydrogen and temperature effects presented in Part 1, and consequently the single crystal recognizes the presence of pentene rather weakly. In contrast to this, on the foil (Fig. 4) the absolute amounts of C–Pd

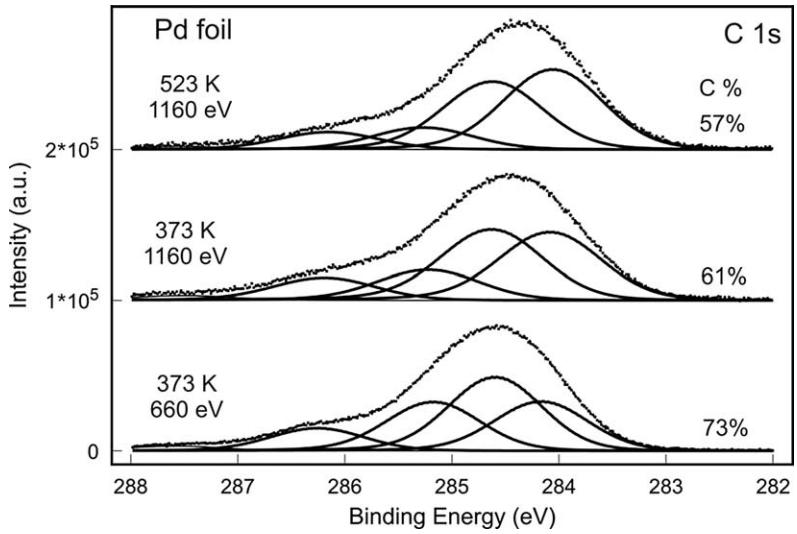

Fig. 5. C1*s* region of Pd foil at higher incident photon energy (1160 eV) in the reaction mixture at 373 and 523 K, compared to the 373 K spectrum taken at 660 eV. (- - -) measured data; (—) fits.

and C–H were much higher at all temperatures. In addition, the spectrum obtained before the introduction of the reaction mixture (1) clearly indicates the thorough transformation of the carbonaceous deposits. From RT to 373 K (when the activity increases), C–H becomes slightly higher and C–Pd slightly lower. Interestingly, the C1*s* region (at an excitation energy of 660 eV) reveals no changes coming from 373 to 523 K, although the catalytic activity disappears. No additional carbonization occurs that might give rise to activity loss. However, a comparison of the foil with the single crystal shows that the foil in the reaction mixture does not follow the tendencies observed for hydrogen. No disappearance of C–H and no increase in C–Pd were obtained. Please note as well that the total carbon content of the foil was rather high ($\sim$ 70%). A very rough calculation of one monolayer of carbon on palladium would give about 45% carbon content for the applied excitation energy, assuming an exponential decay of information with depth. Therefore, as a first approximation, we can consider a full surface coverage; however, the situation is far more complex, since the relative position of carbonaceous species (3D islands, on/in/sub-surface) and their abundance would drastically affect and complicate the calculation.

The corresponding Pd3*d* spectra in the reaction mixture (not shown) reveal a very similar pattern, as already discussed in Part I. (The fitting analysis supplied no clean surface palladium, and the spectra were thus fitted by two components, bulk palladium and adsorbate-induced surface Pd.) The tendencies here are similar to those found for the experiment in pure hydrogen, where the surface-related component decreased with increasing temperature. This effect was more dominant on the Pd(111) single crystal than on the foil.

One of the essential advantages of using a synchrotron as an X-ray source is the opportunity to vary the incident photon energy and hence the KE of the photoelectrons. This allows us to perform depth-profiling experiments. Fig. 5 gives a comparison of the C1*s* spectrum excited with 660-eV photons (= KE $\sim$ 370 eV) with measurements obtained with higher photon energy (1160 eV). The inelastic mean free path for 370-eV KE electrons in C is $\sim$ 13 Å, and for 870-eV electrons ($h\nu = 1160$ eV) it is about 24 Å [46]. A comparison of the 373 K spectra shows that the C–Pd component is higher and the C–H component is lower at higher incident photon energy, meaning that the C–H component is situated above the C–Pd component, with the C–C component in the middle. This indicates that C–Pd is located partly in the palladium surface and in the subsurface region, in good agreement with the suggestions in Part 1. The distribution of the C1*s* species supports our C1*s* peak assignment as well. At higher photon energy the surface sensitivity decreases, that is, the total carbon/palladium ratio is reduced (C%: 73 vs 61%). Comparing the two upper spectra in Fig. 5 (hν 1160 eV at 373 and 523 K), we do see some minor differences between the active (373 K) and inactive (523 K) states of the sample (there was no difference when we used 660-eV excitation; see Fig. 4). At 523 K the C–Pd component is more pronounced, which indicates that the interaction of palladium and carbon is stronger.

Fig. 6 depicts the valence band of the Pd foil and the single crystal at 373 K, in the reaction mixture, that is, when the foil had its highest activity and the single crystal was inactive. The *d*-band of the foil is distinctly narrower and its center is shifted toward the Fermi edge when compared with the single crystal. This change in the electron density in the valence region might contribute to the presence or lack of catalytic activity of palladium.

4. Discussion

The hydrogenation of *trans*-2-pentene was investigated with high-pressure XPS. In the previous section we showed

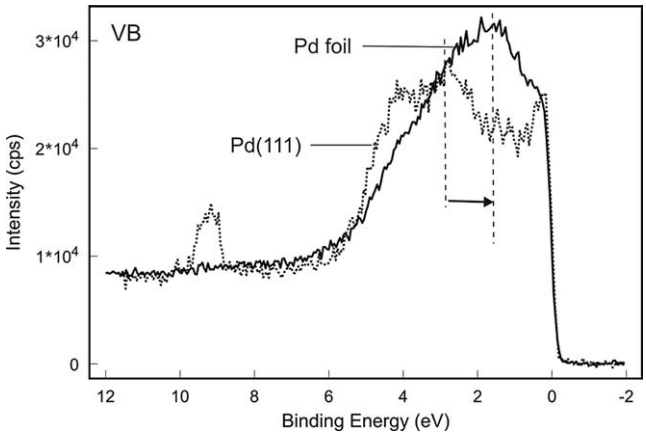

Fig. 6. Valence band spectra of Pd(111) (- - -) and Pd foil (—) in the reaction mixture (0.6 mbar H_2 + 0.2 mbar t-2-p) at 373 K.

that whereas the single crystal was inactive at all the temperatures applied, the polycrystalline foil was active already at room temperature, with a maximum activity at 373 K and a loss of activity at 523 K. In the C1*s* region we found different types of carbonaceous deposits, as was discussed in Part I, and the t-2-p gas-phase peak was also observed. Photon-dependent depth profiling supported the assignment of the C1*s* peaks to different carbon species. Rather remarkably, the total carbon content of the active sample was 70–80%, but only half of that was observed on the inactive single crystal. The amount of graphitic deposit was just slightly (×1.1–1.6) higher on Pd foil compared with single crystal. On the other hand, C–Pd and C–H were much more abundant (×4–10) on the foil. The hydrogen coverage and the amount of solved hydrogen should be on the same order of magnitude for the two samples. According to the palladium/hydrogen phase diagram [47,48], the samples at room temperature should be in the α hydride phase. At 523 K, however, the hydrogen concentration on the surface and in the bulk (subsurface) should dramatically decrease.

In what follows we attempt to answer three questions: What causes the different activities of foil and single crystal? What contributes to the observed activity difference at different temperatures on the Pd foil? How does t-2-p chemisorb on palladium?

Doyle et al. [44] investigated t-2-p hydrogenation under UHV conditions by TDS on thin film-deposited Pd nanoparticles and on Pd(111). The authors found pentane desorption only on the nanoparticles and not on Pd(111). It was concluded that the accessibility of subsurface hydrogen should be the key parameter governing the hydrogenation. Hydrogen/deuterium TDS measurements [20,35,49–51] on different palladium surfaces reveal a rather general pattern for hydrogen species, with differences on the order of a factor of 2–10 in the ad(ab)sorption capacity. The presence or absence of different hydrogen species was mainly governed by the amount and temperature of hydrogen exposure and the prehistory of the samples. Introduction of a macroscopic amount (mbar) of hydrogen, in contrast to the exposure to just some Langmuir of H_2, populates the available surface and subsurface sites to such an extent that the inactivity of the single crystal under mbar conditions cannot be caused by the lack of a particular hydrogen type. (Both of our samples were exposed to hydrogen before the introduction of t-2-p.) Since we performed the same measurements with the same hydrogen pressure and temperature on both samples, we believe that it is not hydrogen availability that causes the difference in the catalytic activity of our samples. In addition, the higher carbon content on the Pd foil might represent a higher energetic barrier for hydrogen entering the foil compared with Pd(111). A major difference is found in the valence band spectra of the samples, where the active Pd foil shows an upshift of its *d*-band—relative to the *d*-band center of Pd(111)—toward E_F. The reasons for the *d*-band shift could be variations in the electron density caused by morphological changes (reduced Pd coordination) and the interaction of palladium with nonstoichiometric species such as carbon [22,52,53]. As was shown before [54–56], the position of the *d*-band center can be correlated with the chemisorption strength of an adsorbate and therefore with the reactivity of the system. Other differences between the foil and the single-crystal sample are their abilities to interact with carbon, to hydrogenate surface carbon, and to maintain the hydrogen-rich (chemisorbed) state. This can be concluded from the higher absolute amount of C–Pd and C–H components on Pd foil in a gaseous atmosphere as compared with the single crystal. As the C–Pd component was assigned to in/subsurface carbon, the much higher C–Pd component on the foil would indicate a much stronger distortion of the palladium lattice (see next paragraph). Interaction of the palladium with carbonaceous entities that are not directly involved in the main reaction can perturb the initial (inactive) state and change the dehydrogenation strength of Pd and thus promote a modified chemisorption strength of t-2-p. We think that the *d*-band position and the different ability to interact with carbon are interconnected, and therefore both are indicators for the activity.

To understand more complex (selective) hydrogenation, our intention was to increase chemical complexity step by step, starting from a single hydrogenation (t-2-p) and then moving toward systems with multiple functionalities. As a second step, 1-pentyne was used because of the possibility of partial and total hydrogenation. In a forthcoming paper [57] we will give a detailed report of that study, with a focus on the morphological changes observed with the palladium foil that was removed from the experimental cell after the reaction. In that system, we also observed by XPS very high carbon content, which apparently did not cause any activity decrease. A representative HRTEM image is shown in Fig. 7. The high-resolution imaging of the "postreaction" Pd surface revealed in numerous places graphitic structures of up to 10 or 12 graphene layers directly on the Pd surface. The graphitic nature is confirmed by the (002) lattice fringes of the graphene layers with spacing of 0.335–0.355 nm. In a very few cases weaker (100) and (102) graphite lattice

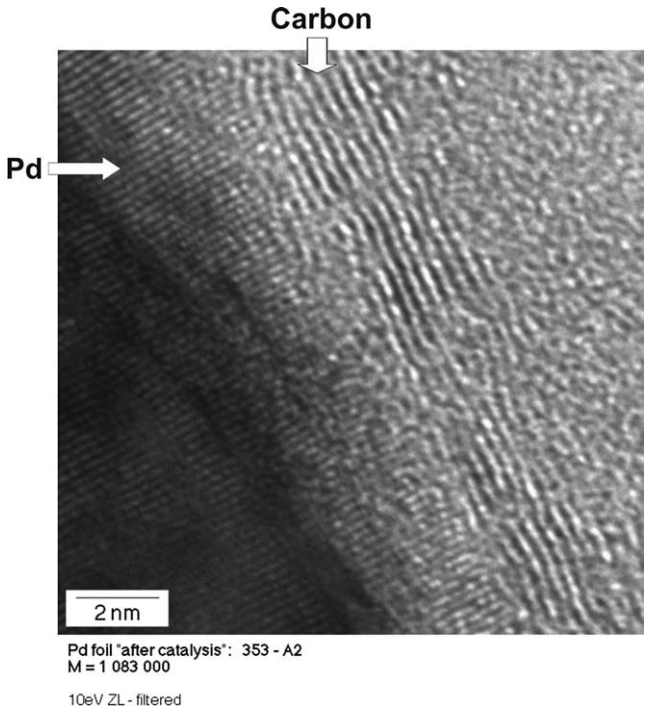

Fig. 7. High resolution TEM image of a Pd foil taken out of our in situ XPS set-up. The sample was used prior the microscopic investigation in the hydrogenation of 1-pentyne.

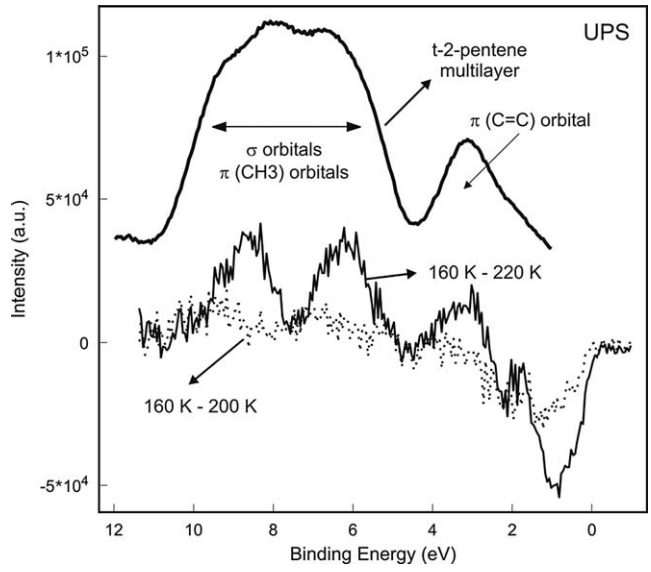

Fig. 8. He I UPS spectra (after background subtraction) of multilayer of t-2-p on Pd(111). Difference spectra (160–200 K and 160–220 K) of the chemisorbed layer on Pd(111).

fringes were also detected, indicating a higher degree of graphitic order in small regions. On the left side (111) lattice fringes of the Pd surface are clearly visible. (Note that the sample was the same type of palladium foil as was used in the *trans*-2-pentene study.) Pd (111) lattice fringes near the surface seem to be expanded by a few percent in comparison with Pd bulk values. This expansion can be explained by carbon incorporation into the palladium lattice. This incorporated, subsurface type of carbon would fit very well with the C–Pd XPS feature and would indicate that a certain degree of lattice distortion is needed to create active centers for hydrogenation reactions.

We will now discuss the effect of temperature on the catalytic activity of the Pd foil (Fig. 2). The Pd foil was active at RT; its activity increased at 373 K and vanished at 523 K. Since we observed no additional reaction path at 523 K and no further carbonization, the blocking of active centers by carbonaceous species can be ruled out as a possible explanation for the deactivation at 523 K. Palladium was most likely in α phase at RT [47,48], and as the temperature increased the reaction rate increased (Arrhenius term) as long as hydrogen was available. TDS measurements made on different palladium surfaces [20,35,49–51] show hydrogen desorption mainly in the temperature range of 150–400 K, depending on the initial exposure temperature. The hydrogen partial pressure in our experiment (0.6 mbar in the presence of 0.2 mbar pentene) might not be high enough to populate at elevated temperature the available ad(ab)sorption sites, and therefore the Pd/C/H equilibrium shifts toward the energetically more favorable carbon-palladium interaction. This can be deduced from the slightly higher C–Pd component at 523 K (as compared with 373 K) in the depth profiling experiment (Fig. 5). The C–H component at 523 K was still observed, indicating no strong dehydrogenation of the chemisorbed overlayer (no loss of hydrogen from carbon). We conclude that under this condition chemisorbed t-2-p is still present on the surface, and therefore at higher temperatures the availability of active hydrogen is rate limiting.

Regarding our third question about the chemisorption geometry of *trans*-2-pentene on palladium, we performed UPS measurements of adsorbed t-2-p on Pd(111). *trans*-2-Pentene was adsorbed on Pd(111) at 100 K. Multilayer adsorption was achieved with 50 Langmuir of t-2-p (Fig. 8, upper curve). The UPS spectrum of the multilayer is similar to the gas-phase spectrum of *trans*-2-butene [58], showing π and σ contributions (no gas-phase UPS of t-2-p is available in the literature). Because of strong desorption in the temperature range of 100–160 K, only a chemisorbed monolayer was present at $T > 160$ K. A TDS measurement by Doyle et al. [44] reveals molecular desorption from the weakly bound multilayer at ~ 130 K and desorption from π-bonded species at ~ 170 K. In addition, a third peak (~ 270 K) was also present, corresponding to σ-bonded pentene molecules. In our experiment we observed no changes in the UPS spectra up to 220 K; thus we believe that the species corresponding to the second TDS peak in Ref. [44] (assigned to π-bonded t-2-p) is also desorbed. However, the spectra of the chemisorbed species were rather comparable to the physisorbed t-2-p, indicating no dramatic alteration of the molecule during chemisorption. As the multilayer desorbs the palladium d-band evolves and overlaps strongly with the π orbital of t-2-p. This overlap makes it difficult to unambiguously identify the presence of the π orbital in the original spectra. However, the use of difference spectra can

clear up this question. At 220 K the UPS spectrum changed dramatically as the π orbital and some contribution from the $\sigma/\pi(CH_3)$ region were removed (160 to 220 K curve). Furthermore, the difference spectrum (160–200 K) clearly indicates that the π orbital is present up to 200 K. From this we conclude that t-2-p changes its chemisorption modus at $\sim$ 210–220 K. The combination of UPS and TDS [44] reveals that, as the π-bonded molecules desorb, there is still σ-bonded t-2-p on the surface. The π bond is intact; therefore the chemisorption occurs via with the loss of hydrogen (probably in position 2 or 3). At $\sim$ 220 K the molecule loses the double bond, and consequently the bonding to the surface changes as well. However, the molecule still can desorb as t-2-p (the third TDS peak at $\sim$ 270 K); therefore the changes should not be irreversible. The same adsorption behavior (TDS) was found on the Pd(111) single crystal and on supported Pd clusters. The latter were active in the hydrogenation of t-2-p (pentane desorption). The result of our UPS experiments is that t-2-p reacts with hydrogen in σ-bonded chemisorption modus, at least in UHV conditions. Whether this chemisorption modus is transferable to realistic pressures will require further investigations to determine.

5. Conclusion

The hydrogenation of *trans*-2-pentene was investigated on palladium foil and Pd(111) single crystal by combined high-pressure XPS and MS analysis. We found activity on the polycrystalline foil sample (RT, 373 K) in the presence of a huge amount (up to 70%) of carbon at an information depth of about 1 nm. Pd(111) was inactive, and its carbon content was about 40%. The different activities of the two samples were related to their *d*-band position in the valence band and the widely different distributions of carbonaceous species. The importance of lattice expansion by carbon incorporation was addressed. The foil sample lost its activity at 523 K, most likely because of hydrogen desorption. Separate UPS measurements revealed that adsorbed t-2-p loses its double bond at about 210 K, and therefore it is the σ-bonded chemisorbed species that is the intermediate of this hydrogenation, at least under UHV conditions.

Acknowledgments

Financial support from the ATHENA Project is gratefully acknowledged. One of us also thanks the Humboldt Foundation for the Roman-Herzog-Stipendium. The authors thank A. Klein-Hoffmann for making the cross-sectional specimen used for HRTEM. In addition, we thank the BESSY staff for their continual support during the XPS measurements.

References

[1] R.A. Dalla Betta, K. Tsurumi, Shoji, US Patent 5258349 (1993).
[2] S. Morikawa, S. Samejima, M. Yoshitake, N. Tatematsu, Jpn Patent 3-099026 (1991).
[3] J. Moore, J. O'Kell, EU Patent 508660 (1992).
[4] A. Chauvel, G. Lefebvre, Petrochem. Proces. 2 (1989) 36.
[5] Hoechst, EP 330853 (1989), EP 403950 (1990), EP 431478 (1991), EP 519435 (1992).
[6] R.B. Anderson, K.C. Stein, J.J. Feenan, L.E.J. Hofer, Ind. Eng. Chem. 53 (1961) 809.
[7] W.K. Lam, L. Lloyd, Oil Gas 27 (1972) 66.
[8] G.C. Bond, P.B. Wells, Adv. Catal. 15 (1964) 91.
[9] T. Mallat, A. Baiker, Catal. Today 19 (1994) 247.
[10] M.L. Derrien, Stud. Surf. Sci. Catal. 27 (1986) 613.
[11] D. Stacchiola, S. Azad, L. Burkholder, W.T. Tysoe, J. Phys. Chem. B 105 (2001) 11233.
[12] B. Heinrichs, J.-P. Schoebrechts, J.-P. Pirard, J. Catal. 200 (2001) 309.
[13] G.B. Hoflund, H.A.E. Hagelin, J.F. Weaver, G.N. Salaita, Appl. Surf. Sci. 205 (2003) 102.
[14] C.F. Cullis, B.M. Willatt, J. Catal. 83 (1982) 267.
[15] J.H. Kang, E.W. Shin, W.J. Kim, J.D. Park, S.H. Moon, J. Catal. 208 (2002) 310.
[16] W.-J. Shen, Y. Ichihashi, H. Ando, Y. Matsumara, M. Okumura, M. Haruta, Appl. Catal. A 217 (2001) 231.
[17] A. Trovarelli, Catal. Rev.-Sci. Eng. 38 (1996) 439.
[18] G. Tourillon, A. Cassuto, Y. Jugnet, J. Massardier, J.C. Bertolini, J. Chem. Soc., Faraday Trans. 92 (1996) 4835.
[19] A. Sandell, A. Beutler, A. Jaworowski, M. Wiklund, K. Heister, R. Nyholm, J.M. Andersen, Surf. Sci. 415 (1998) 411.
[20] U. Muschiol, P.K. Schmidt, K. Christmann, Surf. Sci. 395 (1998) 182.
[21] Sh. Shaikhutdinov, M. Heemeier, M. Bäumer, T. Lear, D. Lennon, R. Oldman, S.D. Jackson, H.-J. Freund, J. Catal. 200 (2001) 330.
[22] D.R. Lloyd, C.M. Quinn, N.V. Richardson, Surf. Sci. 63 (1977) 174.
[23] S. Surnev, M. Sock, M.G. Ramsey, F.P. Netzer, M. Wiklund, M. Borg, J.N. Andersen, Surf. Sci. 470 (2000) 171.
[24] J. Horiuti, M. Polanyi, Trans. Faraday Soc. 30 (1934) 1164.
[25] T.P. Beebe, J.T. Jr. Yates, J. Am. Chem. Soc. 108 (1986) 663.
[26] G.A. Somorjai, G. Rupprechter, J. Phys. Chem. B 103 (1999) 1623.
[27] G. Rupprechter, G.A. Somorjai, Catal. Lett. 48 (1997) 17.
[28] S.T. Ceyer, Acc. Chem. Res. 34 (2001) 737.
[29] A. Sárkány, J. Chem. Soc., Faraday Trans. I 84 (1988) 2267.
[30] A. Sárkány, J. Catal. 180 (1998) 149.
[31] Z. Paál, J. Mol. Catal. 94 (1994) 225.
[32] P.G. Menon, J. Mol. Catal. 59 (1990) 207.
[33] A.S. Al-Ammar, G.J. Webb, J. Chem. Soc., Faraday Trans. I 74 (1978) 195.
[34] S.D. Jackson, N.J. Casey, J. Chem. Soc., Faraday Trans. I 91 (1995) 3269.
[35] Sh. Shaikhutdinov, M. Frank, M. Bäumer, S.D. Jackson, R.J. Oldman, J.C. Hemminger, H.-J. Freund, Catal. Lett. 80 (2002) 115.
[36] M. Kaltchev, D. Stacchiola, H. Molero, G. Wu, A. Blumenfeld, W.T. Tysoe, Catal. Lett. 60 (1999) 11.
[37] F. Zaera, Mol. Phys. 100 (2002) 3065.
[38] J.A. Gates, L.L. Kesmodel, Surf. Sci. 124 (1983) 68.
[39] W.T. Tysoe, G.L. Nyberg, R.M. Lambert, J. Phys. Chem. 90 (1986) 3188.
[40] B. Hugenschmidt, P. Dolle, J. Jupille, A. Cassuto, J. Vac. Sci. Technol. A 7 (1989) 3312.
[41] H. Siegbahn, J. Phys. Chem. 89 (1985) 897.
[42] H. Bluhm, I. Posvirin, M. Hävecker, A. Knop-Gericke, D. Teschner, E. Kleimenov, A. Pestryakov, R. Schlögl, V.I. Bukhtiyarov, in preparation.
[43] T. Karlsen, L.J. Saethre, K.J. Borve, N. Berrah, E. Kukk, J.D. Bozek, T.X. Carroll, T.D. Thomas J. Phys. Chem. A 105 (2001) 7700.
[44] A. Doyle, Sh. Shaikhutdinov, S.D. Jackson, H.-J. Freund, Ang. Chem. 42 (2003) 5240.

[45] As the C1*s* spectra were scaled up to the same height, the relative intensity of the gas phase peak varies. The higher the quantity of surface carbon the lower will be the gas phase signal, thus the major difference in relative height of the gas phase peaks comes from this scaling procedure. Nevertheless, the intensity of the gas phase signal depends also on the width of the gas phase irradiated by the X-ray between the sample and the first aperture. Consequently, on the distance of the sample from the aperture. This distance might be not exactly the same for the two samples, contributing to the differences in the relative intensity of the gas phase signal seen in Fig. 3 and Fig. 4. Note that mechanical stress in the heating stage moves also the sample (and its surface) relative to the first aperture; therefore the height of the gas phase peak might not be constant at different temperatures.
[46] S. Tanuma, C.J. Powell, D.R. Penn, Surf. Interface Anal. 17 (1991) 911.
[47] H. Frieske, E. Wicke, Ber. Bunsenges. 77 (1973) 48.
[48] R.J. Wolf, M.W. Lee, R.C. Davis, P.J. Fay, J.R. Ray, Phys. Rev. B 48 (1993) 12415.
[49] M. Wilde, M. Matsumoto, K. Fukutani, T. Aruga, Surf. Sci. 482–485 (2001) 246.
[50] H. Okuyama, W. Siga, N. Takagi, M. Nishijima, T. Aruga, Surf. Sci. 401 (1998) 344.
[51] G.E. Gdowski, T.E. Felter, R.H. Stulen, Surf. Sci. 181 (1987) L147.
[52] W. Olovsson, E. Holmström, A. Sandell, I.A. Abrikosov, Phys. Rev. B 68 (2003) 045411.
[53] A. Sellidj, B.E. Koel, Phys. Rev. B 49 (1994) 8367.
[54] B. Hammer, J.K. Norskov, Adv. Catal. 45 (2000) 71.
[55] B. Hammer, Y. Morikowa, J.K. Norskov, Phys. Rev. Lett. 76 (1996) 2141.
[56] J.A. Rodriguez, D.W. Goodman, Science 257 (1992) 897.
[57] D. Teschner, E. Kleimenov, A. Pestryakov, M. Hävecker, A. Knop-Gericke, R. Schlögl, in preparation.
[58] K. Kimura, S. Katsumata, Y. Achiba, T. Yamazaki, S. Iwata, in: Handbook of HeI Photoelecrton Spectra of Fundamental Organic Molecules, Japan Scientific Societies Press, Tokyo, 1981, p. 60.